Title

Dynamic tumor-tracking radiotherapy with real-time monitoring for liver tumors using a gimbal mounted linac

Authors

Yusuke Iizuka[1], Yukinori Matsuo[1], Yoshitomo Ishihara[1], Mami Akimoto[1], Hiroaki Tanabe[2], Kenji Takayama[2], Nami Ueki[1], Kenji Yokota[1], Takashi Mizowaki[1], Masaki Kokubo[2, 3], Masahiro Hiraoka[1]

[1]Department of Radiation Oncology and Image-applied Therapy, Kyoto University Graduate School of Medicine, Kyoto, Japan

[2]Division of Radiation Oncology, Institute of Biomedical Research and Innovation, Kobe, Japan

[3]Department of Radiation Oncology, Kobe City Medical Center General Hospital, Kobe, Japan

Corresponding Author

Yukinori Matsuo

ymatsuo@kuhp.kyoto-u.ac.jp

54 Kawahara-cho, Shogoin Sakyo-ku, Kyoto 606-8507, Japan

Phone +81-75-751-3419

Running title

Dynamic tumor-tracking SBRT for liver tumors

Keywords

Dynamic tumor tracking, Real-time monitoring, Liver tumor.

Conflicts of interest

Takashi Mizowaki, Masaki Kokubo, and Masahiro Hiraoka have a consultancy agreement with Mitsubishi Heavy Industries, Ltd., Japan. Kenji Yokota is loaned employee from Mitsubishi Heavy Industries, Ltd.

Acknowledgement

This research was partially supported by the Practical Research for Innovative Cancer Control (15ck0106035h0002) from Japan Agency for Medical Research and Development (AMED). The funding program had no effect on the study design or the interpretation of data.

Abstract

Purpose

Dynamic tumor-tracking stereotactic body radiotherapy (DTT-SBRT) for liver tumors with real-time monitoring was carried out using a gimbal-mounted linear accelerator and the efficacy of the system was determined. In addition, four-dimensional (4D) dose distribution, tumor-tracking accuracy, and tumor-marker positional variations were evaluated.

Materials and methods

A fiducial marker was implanted near the tumor prior to treatment planning. The prescription dose at the isocenter was 48–60 Gy, delivered in four or eight fractions. The 4D dose distributions were calculated with a Monte Carlo method and compared to the static SBRT plan. The intrafractional errors between the predicted target positions and the actual target positions were calculated.

Results

Eleven lesions from ten patients were treated successfully. DTT-SBRT allowed an average 16% reduction in the mean liver dose compared to static SBRT, without altering the target dose. The average 95th percentiles of the intrafractional prediction errors were 1.1, 2.3, and 1.7 mm in the left-right, cranio-caudal, and anterior-posterior directions, respectively. After a median follow-up of 11 months, the local control rate was 90%.

Conclusions

Our early experience demonstrated the dose reductions in normal tissues and high accuracy in tumor tracking, with good local control using DTT-SBRT with real-time monitoring in the treatment of liver tumors.

Manuscript

Introduction

While hepatocellular carcinoma (HCC) is the most common primary liver cancer [1], the liver is also a frequent site of metastases from other tumors, especially those of the gastrointestinal tract. Clinical guidelines recommend surgical resection, liver transplantation or radiofrequency ablation (RFA) to treat localized HCC in patients with good hepatic function. However, only 10–30% of patients with HCC or liver metastases are candidates for tumor resection, mainly because of their poor hepatic function. Furthermore, RFA cannot be applied for primary or metastatic tumors larger than 3 cm, near vessels, the intestines, or the biliary system nor can it be used to treat tumors not reached under ultrasonography or computed tomography (CT) guidance [2,3].

Stereotactic body radiotherapy (SBRT) provides excellent local control of liver tumors and is thus recognized as an alternative therapy for patients with liver tumors not suitable for resection or RFA [4-8]. However, because the liver moves during the respiratory cycle, if respiratory motion is not appropriately managed, normal liver tissue will be unintentionally included in the irradiation field.

The American Association of Physicists in Medicine Task Group 76 proposed five methods to control motion: motion-encompassing, respiratory-gating, breath-hold, forced shallow breathing with abdominal compression, and real-time tumor-tracking [9]. Among these, real-time tumor-tracking is recognized as the optimum method of managing respiratory motion with respect to the normal tissue irradiation dose, treatment time, and patient compliance.

In this study, we applied dynamic tumor-tracking (DTT) SBRT to liver tumors and evaluated four-dimensional (4D) dose distribution, tumor-tracking accuracy, and positional variations between the tumor and the fiducial marker during the respiratory cycle.

Materials and methods

Patients

Eligibility criteria for this study were as follows: (1) one or two liver tumors with a diameter ≤50 mm, (2) patients medically unfit for surgical resection or percutaneous ablation, or who refused these therapies, (3) Eastern Cooperative Oncology Group performance status [10] of 0–2, (4) Child-Pugh score ≤8, and (5) written informed consent. This study was carried out in Kyoto University Hospital (KU; Kyoto, Japan) and Institute of Biomedical Research and Innovation (IBRI; Kobe, Japan), and approved by our Institutional Review Boards

Treatment system

We used the Vero4DRT system (formerly called MHI-TM2000; Mitsubishi Heavy Industries Tokyo, Japan, and BrainLab, Feldkirchen, Germany) v.3.1.6 for this study. Mechanical details of the Vero4DRT system have been described [11].

Our tumor-tracking is based on a pre-built 4D model, which correlates the internal tumor position with an external respiratory signal. The internal tumor positions are determined via implanted fiducial marker detected with the kV X-ray imaging

subsystems. The respiratory signals are acquired with an infra-red (IR) camera that monitors the IR markers on the patient's abdominal wall. [12, 13]

Pre-planning procedures

Before treatment planning, a gold coil marker (Visicoil, IBA dosimetry, Louvain-la-neuve, Belgium) was inserted near the tumor [14]. Planning CTs were acquired 1 week after insertion of the marker.

Two sets of 4DCT (non-contrast and contrast-enhanced) and two or three sets of breath-hold CT at exhale were acquired for treatment planning using a 16-slice CT scanner. The non-contrast 4DCT images were used to calculate the monitor units (MUs), to avoid an influence of contrast medium, and the contrast-enhanced 4DCT images were used for delineation of target volumes. After CT scanning, a 4D model was built to evaluate mean and standard deviation (SD) in errors between detection and prediction from the 4D model, and to evaluate tumor motion amplitude using the ExacTrac subsystem. The detailed protocols for the Visicoil insertion and CT acquisition are described in the Supplementary materials section.

Treatment planning

The non-contrast breath-hold CT and the end-exhale phase from the non-contrast 4DCT were used as a reference CT at IBRI and KU, respectively. Gross tumor volumes (GTVs) were delineated on the contrast-enhanced breath-hold CT scans and on the 10-phase images from the contrast-enhanced 4DCT scans using iPlan RT image (v4.1;

BrainLab). When the tumors were difficult to identify on the planning CTs, the images were fused with diagnostic CT or magnetic resonance images (MRI) based on anatomical landmarks. An internal target volume for tumor-tracking (ITVtracking) was defined as a composite of the GTVs from the breath-hold CT and the ten-phase images from 4DCT that were superimposed onto the reference CT, with translation of the mid-point of the Visicoil to be matched. The ITVtracking was supposed to compensate influence of tumor deformation, positional error due to the fiducial marker rotation, and uncertainty in the positional relationship between the tumor and fiducial marker during respiration. The planning target volume for tumor-tracking (PTVtracking) was defined as the ITVtracking plus additional margins of 5 mm or larger in each direction. The additional margins were defined individually for each patient. An offset vector between the tumor and the mid-point of the Visicoil was determined on the reference CT, which was transferred to ExacTrac system. The offset vector was assumed to be constant and was applied to all treatment fractions. A static SBRT plan, based on the motion-encompassing method, was prepared as a backup in case tracking irradiation could not be applied. ITV for the motion-encompassing method (ITVbackup) was defined as a simple composite of GTVs from the breath-hold CT and the 4DCT without CT center translation. For the PTV for static irradiation (PTVbackup), a 5-mm margin expansion was applied to the ITVbackup in each direction. We describe and illustrate the definition of these targets in detail in the Supplementary material section.

The reference CT image set was used for dose calculation in the tracking plan, and an average image from the 4DCT was used for the static plan. The dose distributions were

calculated using the X-ray voxel Monte Carlo algorithm in iPlan RT dose (v4.5; BrainLab).

The prescribed dose was 48–60 Gy, delivered in 4–8 fractions at the isocenter in both the DTT and the static plans. The multi-leaf collimator was shaped to the PTV plus 0- to 5-mm and adjusted manually to fit the 80% isodose line to the PTV edge and follow dose constrains of the liver or other organs at risk (OARs). The dose constraints in our hospitals are shown in Table 1. Seven to nine static non-coplanar ports of the 6-MV beam were arranged, with a dose rate of 500 MU/min. Intensity modulated radiotherapy (IMRT) was not used in this study.

An in-house-developed software was used to compare dose distributions between the DTT and the static plans. The software can calculate dose distribution based on a Monte Carlo simulation and by considering the gimbal head rotation which was determined by the offset vector and the position of fiducial marker [15,16]. Doses were calculated for each phase from the non-contrast 4DCT in the both plans without dose accumulation and evaluated statistically by paired t-test, after these values were assured to follow a normal distribution. The target and OAR volumes were transferred from the contrast-enhanced 4DCT and modified manually. When the dose-volume metrics in the DTT plan were better than those in the static plan, we decided to apply the DTT irradiation to the patient.

Beam delivery and evaluation of accuracy

The patient was placed in supine position on the vacuum pillow and set-up error was

corrected. Then, a 4D model was built for the treatment fraction. During irradiation, the position of the Visicoil was monitored visually using the kV X-ray imagers every second through the console display to ascertain the irradiation was performed accurately (Supplementary Fig. 2) [17].

The evaluation of intrafractional prediction error and positional variation was carried out after the treatment was finished in each patient in the same way as in the lung tumor [18,19]. The details are described in the Supplementary material section.

Results

Twelve patients were enrolled between February 2013 and April 2014. Their characteristics are summarized in Table 2. For all patients, the Visicoil was placed successfully near the tumor without complication. Two patients were not treated with DTT-SBRT. In one of these patients (patient 2), respiratory motion was so small (<5 mm) that we chose to perform the motion-encompassing SBRT instead. In the other patient (patient 5), a tumor thrombosis was detected at the planning CT and the SBRT was canceled. In this study, eleven tumors in the remaining ten patients were treated with DTT-SBRT. The mean liver volume was 1168 cm^3 (range, 709–1670 cm^3) and the mean magnitude of the offset vector between the tumor and the mid-point of the Visicoil on the reference CT was 28.0 mm (range, 16.0–49.7 mm) in the ten patients.

Target size and OARs dose exposure reduction

The median peak-to-peak movement of the tumors measured with 4DCT was 2.3, 7.2,

and 4.1 mm in the left-right (LR), cranio-caudal (CC), and anterior-posterior (AP) directions, respectively.

The margin between PTVtracking and ITVtracking in the CC direction was 6.5 mm in three patients (patients 1, 7 and 12) and 5.0 mm in the others. A 5.0 mm margin was applied in the LR and AP directions of all eleven tumors. The mean PTV reduction with DTT was 35% (18–64%) relative to the static plan, based on a mean volume of 73.8 to 47.9 cm^3.

Table 3 shows the exposure of the target volume and the OARs for the DTT and static plans. In all cases, the exposure dose to the liver was lower in the DTT plan than in the static plan, without sacrificing the dose delivered to the target. In a patient with a tumor located near the colon or duodenum, the maximum doses to the intestines were reduced (Supplementary. Fig. 3).

Treatment delivery and accuracy

The planned DTT-SBRT fractions were successfully delivered to the ten patients. The mean treatment time which included patient set-up, building the 4D model, and beam delivery was 28 min (range, 17-48 min) for all 68 fractions (Supplementary Table 1).

According to the log file analysis, the average 95th percentiles of the absolute value of the intrafractional prediction errors were 1.1, 2.3, and 1.7 mm in the LR, CC, and AP directions, respectively. The root mean square (RMS) in the intrafractional variation between the tumor and the fiducial marker were 0.9, 1.2, and 1.5 mm in the LR, CC, and AP directions, respectively. The detailed results about treatment accuracy and

intrafractional variation are shown in the Supplementary materials section.

Clinical outcome and adverse events

During a median follow-up period of 11 months (range, 7–21 months), one patient developed local recurrence within the irradiation field at 4 months after DTT-SBRT (patient 3). The one-year local control rate was 90%. There was one case of liver metastases at 15 months after DTT-SBRT (patient 1). No treatment-related toxicity of grade 4 or worse was observed. Grade 3 liver enzyme elevation and grade 2 biliary enzyme elevation were observed in a patient (patient 8) a month after DTT-SBRT. These enzymes decreased to their pre-treatment levels next month without any medication.

Discussion

This is the first study to report both dosimetric advantage and clinical outcomes in liver tumor patients treated with DTT-SBRT using the Vero4DRT system. The successful use of DTT-SBRT for liver tumors demonstrated in this study suggests that the decrease in OAR doses with this approach is likely to translate into a reduction of adverse events [20]. The prevention of adverse events after liver SBRT requires a reduction in the dose to normal tissue surrounding the target. Although definitive dose constraints for liver SBRT have yet to be determined [21, 22], a mean liver dose of <15 Gy and a spared V15 (the volume receiving ≤15 Gy) of >700 cm^3 have been proposed [5, 23]. In this study, the DTT method reduced the mean liver dose from 11.5 Gy to 9.7 Gy and

increased the spared V15 from 786 cm^3 to 910 cm^3 ($p < 0.01$) compared to static SBRT, without compromising the dose to the target volume. The patients in the present study had a small liver volume (mean of 1168 cm^3) because of previous operations or pre-existing cirrhosis. In three patients a spared V15 >700 cm^3 was achieved with DTT-SBRT, but would not have been achievable with static SBRT. The intestine, colon, and spinal cord are the other OAR in liver SBRT, and strict constraints on the maximal dose must therefore be maintained [21]. The DTT approach potentially reduces the doses to these organs, as was the case in patient 4 (Supplementary Fig. 3). With the DTT method, SBRT applications can be extended to tumors that emerge in patients with a small liver or near such critical organs as the intestine, colon, and spinal cord. Depuydt et al. analyzed 10 patients treated with DTT-SBRT using Vero4DRT, including three with liver tumors [24]. They accumulated doses on multiple phase images from 4DCT onto one phase using a deformable registration technique. They reported an average PTV reduction of 31% and a mean liver dose reduction in patients with liver tumor of 20%. The authors also calculated the normal tissue complication probability of radiation-induced liver disease (RILD) and in one patient estimated a 2.5% reduction treated with the DTT method. Our results that PTV reduction of 35% and a mean liver dose reduction of 16% were similar to theirs. However, we evaluated doses on each phase of the 4DCT images separately without use of deformable registration. Concerning the clinical outcomes, only one patient in this study suffered from a Grade 3 adverse event, which spontaneously regressed without any medication.

Our previous study on tracking error in lung cases showed that prediction error was

much dominant to mechanical error (0.1 and 1.2 mm in the LR, 0.4 and 2.7 mm in the CC, and 0.1 and 2.1 mm in the AP directions, for the mechanical and the prediction errors, respectively) [18]. Based on the result, the present study evaluated the prediction error which was easier to calculate than the total tracking error. The high accuracy in the prediction of the target position was confirmed by the average 95th percentiles of the absolute value of the intrafractional prediction error of 1.1, 2.3, and 1.7 mm in the LR, CC, and AP directions, respectively. These results are comparable with our previous experience in lung DTT as shown above. Our results are also in agreement with those of Hoogeman et al., who used the CyberKnife robotic radiosurgery system with an integrated Synchrony Respiratory Tracking System (Accuray, Sunnyvale, CA) in patients with lung tumors. In that study, the SDs describing the intrafractional prediction error around the whole fraction mean ranged between 0.0–1.3 mm, 0.0–2.9 mm, and 0.0–2.4 mm for the LR, CC, and AP directions, respectively [25].

It should be noted that in all other studies reported thus far, the prediction errors were determined by measuring the position of the fiducial markers, not the tumor position itself, based on the assumption that the relative position between the tumor and the fiducial marker is constant. We evaluated intrafractional positional variation between the tumor and the fiducial marker in patients with liver tumor. The RMS in the intrafractional variation between the tumor and the fiducial marker was 0.9, 1.2, and 1.5 mm in the LR, CC, and AP directions, respectively. These values are similar to those obtained in our lung study of DTT (0.6, 1.5, and 0.9 mm) [19]. In the present study, the intrafractional positional variation was included in the ITVtracking.

For the PTV margin, both the intrafractional prediction error and the interfractional positional variation between the tumor and the fiducial marker were considered. To our knowledge, there are no reports in which the interfractional positional variation between liver tumors and internal fiducial markers was evaluated directly, although in others motion among internal markers in the liver was investigated. There are reports indicated the interfractional fiducial migration was minimal in the liver [26-28]. Since in our study the maximum of the 95th percentiles of the absolute value of the intrafractional prediction error was 4.4 mm, the actually required PTV margin was included in this margin.

There are several reports concerning clinical results of DTT-SBRT using the CyberKnife system. Louis et al. reported the local control rate of 95% at a median follow up of 13 months in 25 patients with HCC. They observed 2 cases of Gr 3 adverse events (pain and hepatic toxicity) [29]. Vautravers-Dewas et al. studied 42 patients with liver metastases. They reported the local control of 90% at median follow up of 14 months with one case of Gr 3 epidermitis [30]. Though the follow up time was short, our clinical results are in accord with them. Besides, if we combine the IMRT with the DTT method, we could extend the application further. A planning study conducted by Chen et al. revealed that IMRT or volumetric modulated arc therapy could lower the risk of RILD compared with 3D conformal radiotherapy [31]. The DTT-IMRT had been applied for pancreas cancer in our institution [32].

There were several limitations in this study. First, the delineation uncertainties of GTVs and fiducial markers in the binned 4DCT affected the results of dose evaluation and

values of intrafractional positional variations between the tumor and the fiducial marker. Though we acquired many series of breath-hold CT, and non-contrast and contrast-enhanced 4DCT to minimize the delineation uncertainties, the timing of image acquisition was not ideal for delineating the GTVs. There were artifacts in the 4DCT due to the respiratory motion and the variation of respiratory motion and period. A more sophisticated technique to determine the tumor position and fiducial marker accurately during free breathing is warranted. A multimodality imaging such as MRI or positron emission tomography [33] and volumetric image acquisition with wide detector CT could be a solution [34, 35]. Second, we did not use a deformable registration to evaluate the 4D dose distribution because dose accumulation with deformable registration includes potential errors that cannot be ignored in abdominal regions [36, 37]. Finally, there were a small number of patients and the short observation period. Long-term clinical outcomes in a larger number of patients and the occurrence of late adverse events remain to be determined.

In conclusion, DTT-SBRT with real-time monitoring showed dose reductions in normal tissues and high accuracy in tumor-tracking, with good local control.

References

[1] Barazani Y, Hiatt JR, Tong MJ, Busuttil RW. Chronic viral hepatitis and hepatocellular carcinoma. World J Surg 2007;31:1243-8.

[2] Kudo M, Izumi N, Kokudo N, et al. Management of hepatocellular carcinoma in Japan: Consensus-Based Clinical Practice Guidelines proposed by the Japan Society of Hepatology (JSH) 2010 updated version. Dig Dis 2011;29:339-64.

[3] Bruix J, Sherman M, American Association for the Study of Liver Disease. Management of hepatocellular carcinoma: an update. Hepatology 2011;53:1020-2.

[4] Hoyer M, Roed H, Traberg Hansen A, et al. Phase II study on stereotactic body radiotherapy of colorectal metastases. Acta Oncol 2006;45:823-30.

[5] Kavanagh BD, Schefter TE, Cardenes HR, et al. Interim analysis of a prospective phase I/II trial of SBRT for liver metastases. Acta Oncol 2006;45:848-55.

[6] Mendez Romero A, Wunderink W, Hussain SM, et al. Stereotactic body radiation therapy for primary and metastatic liver tumors: A single institution phase i-ii study. Acta Oncol 2006;45:831-7.

[7] Takeda A, Sanuki N, Eriguchi T, et al. Stereotactic ablative body radiotherapy for previously untreated solitary hepatocellular carcinoma. J Gastroenterol Hepatol 2014;29:372-9.

[8] Iwata H, Shibamoto Y, Hashizume C, et al. Hypofractionated stereotactic body radiotherapy for primary and metastatic liver tumors using the novalis image-guided system: preliminary results regarding efficacy and toxicity. Technol Cancer Res Treat 2010;9:619-27.

[9] Keall PJ, Mageras GS, Balter JM, et al. The management of respiratory motion in radiation oncology report of AAPM Task Group 76. Med Phys 2006;33:3874-900.

[10] Oken MM, Creech RH, Tormey DC, et al. Toxicity and response criteria of the Eastern Cooperative Oncology Group. Am J Clin Oncol 1982;5:649-55.

[11] Kamino Y, Takayama K, Kokubo M, et al. Development of a four-dimensional image-guided radiotherapy system with a gimbaled X-ray head. Int J Radiat Oncol Biol Phys 2006;66:271-8.

[12] Mukumoto N, Nakamura M, Sawada A, et al. Accuracy verification of infrared marker-based dynamic tumor-tracking irradiation using the gimbaled x-ray head of the Vero4DRT (MHI-TM2000). Med Phys 2013;40:041706.

[13] Matsuo Y, Ueki N, Takayama K, et al. Evaluation of dynamic tumour tracking radiotherapy with real-time monitoring for lung tumours using a gimbal mounted linac. Radiother Oncol 2014;112:360-4.

[14] Vandenbroucke F, Vinh-Hung V, Craggs B, Buls N, de Mey J. Image-guided marker placement in liver tumors for stereotactic radiotherapy: technique and safety. J Comput Assist Tomogr 2010;34:367-71.

[15] Ishihara Y, Sawada A, Nakamura M, et al. Development of a dose verification system for Vero4DRT using Monte Carlo method. J Appl Clin Med Phys 2014;15:4961.

[16] Ishihara Y, Sawada A, Miyabe Y, et al. Four-dimensional Monte Carlo Dose Calculation Method for Dynamic Tumor Tracking Irradiation With a Gimbaled X-ray Head. Int J Radiat Oncol Biol Phys 2012;84:S853-S54.

[17] Akimoto M, Nakamura M, Mukumoto N, et al. Predictive uncertainty in infrared marker-based dynamic tumor tracking with Vero4DRT. Med Phys 2013;40(9):091705.

[18] Mukumoto N, Nakamura M, Yamada M, et al. Intrafractional tracking accuracy in infrared marker-based hybrid dynamic tumour-tracking irradiation with a gimballed linac. Radiother Oncol 2014;111.301-5.

[19] Ueki N, Matsuo Y, Nakamura M, et al. Intra- and interfractional variations in geometric arrangement between lung tumours and implanted markers. Radiother Oncol 2014;110:523-8.

[20] Jung J, Yoon SM, Kim SY, et al. Radiation-induced liver disease after stereotactic body radiotherapy for small hepatocellular carcinoma: clinical and dose-volumetric parameters. Radiat Oncol 2013;8:249.

[21] Sawrie SM, Fiveash JB, Caudell JJ. Stereotactic body radiation therapy for liver metastases and primary hepatocellular carcinoma: normal tissue tolerances and toxicity. Cancer Control 2010;17:111-9.

[22] Timmerman RD. An overview of hypofractionation and introduction to this issue of seminars in radiation oncology. Semin Radiat Oncol 2008;18:215-22.

[23] Pan CC, Kavanagh BD, Dawson LA, et al. Radiation-associated liver injury. Int J Radiat Oncol Biol Phys 2010;76:S94-100.

[24] Depuydt T, Poels K, Verellen D, et al. Treating patients with real-time tumor tracking using the Vero gimbaled linac system: implementation and first review. Radiother Oncol 2014;112:343-51.

[25] Hoogeman M, Prevost JB, Nuyttens J, Poll J, Levendag P, Heijmen B. Clinical accuracy of the respiratory tumor tracking system of the cyberknife: assessment by analysis of log files. Int J Radiat Oncol Biol Phys 2009;74:297-303.

[26] Xu Q, Hanna G, Grimm J, et al. Quantifying rigid and nonrigid motion of liver tumors during stereotactic body radiation therapy. Int J Radiat Oncol Biol Phys 2014;90:94-101.

[27] Kothary N, Heit JJ, Louie JD, et al. Safety and efficacy of percutaneous fiducial marker implantation for image-guided radiation therapy. J Vasc Interv Radiol 2009;20:235-9.

[28] Shirato H, Harada T, Harabayashi T, et al. Feasibility of insertion/implantation of 2.0-mm-diameter gold internal fiducial markers for precise setup and real-time tumor tracking in radiotherapy. Int J Radiat Oncol Biol Phys 2003;56:240-7.

[29] Louis C, Dewas S, Mirabel X, et al. Stereotactic radiotherapy of hepatocellular carcinoma: preliminary results. Technol Cancer Res Treat 2010;9:479-87.

[30] Vautravers-Dewas C, Dewas S, Bonodeau F, et al. Image-guided robotic stereotactic body radiation therapy for liver metastases: is there a dose response relationship? Int J Radiat Oncol Biol Phys 2011;81:e39-47.

[31] Chen D, Wang R, Meng X, et al. A comparison of liver protection among 3-D conformal radiotherapy, intensity-modulated radiotherapy and RapidArc for hepatocellular carcinoma. Radiat Oncol 2014;9:48.

[32] Nakamura A, Mizowaki T, Itasaka S, et al. First implementation of intensity-modulated dynamic tumor-tracking RT in pancreatic cancer using a gimbaled linac. Radiother Oncol. 2014;111:S500.

[33] Brock KK. Imaging and image-guided radiation therapy in liver cancer. Semin Radiat Oncol 2011;21:247-55.

[34] Yamashita H, Kida S, Sakumi A, et al. Four-dimensional measurement of the displacement of internal fiducial markers during 320-multislice computed tomography scanning of thoracic esophageal cancer. Int J Radiat Oncol Biol Phys 2011;79:588-95.

[35] Mori S, Hara R, Yanagi T, et al. Four-dimensional measurement of intrafractional respiratory motion of pancreatic tumors using a 256 multi-slice CT scanner. Radiother Oncol 2009;92:231-7.

[36] Velec M, Moseley JL, Craig T, Dawson LA, Brock KK. Accumulated dose in liver stereotactic body radiotherapy: positioning, breathing, and deformation effects. Int J Radiat Oncol Biol Phys 2012;83:1132-40.

[37] Velec M, Moseley JL, Eccles CL, et al. Effect of breathing motion on radiotherapy dose accumulation in the abdomen using deformable registration. Int J Radiat Oncol Biol Phys 2011;80:265-72.

Tables

Table 1. Dose constraints for organs at risk in our hospitals.

Organ	Dose Constraint
Liver	$V_{20} < 25\%$, spared $V_{15} > 700$ cm^3 (if possible)
Spinal cord	Max dose 25Gy/4fr, 33.5Gy/8fr
Kidneys	$V_{20} < 30\%$
Stomach, Colon	$V_{35} < 1$ cm^3 (4fr), $V_{40} < 1$ cm^3 (8fr)
Duodenum	$V_{28} < 1$ cm^3 (4fr), $V_{35} < 1$ cm^3 (8fr)

Spared V_{15} means the volume receiving ≤15 Gy; V_n: organ volume that receives a dose of n Gy or less; D_n: dose received by n% of organ volume.

Table 2. Patients' characteristics, fractionation schedules, and treatment sites.

Pt	Age	Sex	PS	Histology	Liver volume (cm^3)	Tumor location	Tumor diameter (mm)	Motion amplitude (mm)	Dose/ Fraction (Gy/fr)	OTT (days)
1	72	M	1	Met (lung Ad)	932	S6-7	32	9.7	56/4	9
2	62	M	0	CCC	826	S1	15	1.6	60/8	10
3	64	M	0	CCC	1670	S4	30	1.7	60/8	13
						S7	8	9.0	56/4	12
4	75	F	0	HCC	1479	S7	27	7.1	48/4	4
5	78	F	0	HCC	NA	S7-8	30	NA	NA	NA
6	70	M	0	HCC	1045	S1	28	4.4	56/8	10
7	44	F	0	Met (colon Ad)	1181	S7	16	5.1	56/4	4
8	74	M	0	HCC	1045	S2-3	23	11.4	60/8	9
9	79	F	0	HCC	709	S5	30	16.6	56/8	13
10	69	M	0	HCC	1228	S4	50	7.7	56/8	10
11	55	M	0	Met (lung Ad)	1252	S4	33	5.0	56/8	13
12	88	F	0	HCC	1294	S8	18	7.2	48/4	4

Patient 3 had two lesions. Patient 2 and 4 did not undergo dynamic tumor tracking stereotactic body radiotherapy. Tumor motion amplitude was calculated based on the contrast-enhanced 4DCT.

Abbreviations; Pt: patient, M: male, F: female, PS: performance status, OTT: overall treatment time, Met: metastasis, Ad: adenocarcinoma, HCC: hepatocellular carcinoma, CCC: cholangiocellular carcinoma, NA: not available.

Table 3. Summary of the target size reduction and dose volume evaluation.

	Static	Dynamic tracking	Difference (%)	p-values*
PTV size (cm^3)	73.8 (36.5-133)	47.9 (18.7-91.0)	-35.1	<0.01
GTV D_{95} (%)	94.4 (88.5-99.0)	94.0 (87.2-97.9)	-0.4	0.15
Liver mean dose (Gy)	11.5 (7.1-16.9)	9.7 (5.2-13.3)	-16.2	<0.01
Liver V_{20} (cm^3)	211 (108-361)	168 (83.9-301)	-20.2	<0.01
Normal liver <15 Gy (cm^3)	786 (488-1232)	910 (553-1299)	15.8	<0.01

D_{95} means the dose received by 95% of the target volume. V_{20} means the organ volume that receives a dose of 20 Gy or less; Spared V_{15} means the volume receiving ≤15 Gy;

Abbreviations; PTV: planning target volume, GTV: gross tumor volume.

Values are shown in mean (range).

* p-values by two-sided paired t-test

Supplementary materials

Supplementary document

A fiducial marker insertion and computed tomography (CT) acquisition

Before treatment planning, a gold coil 10 mm in length and 0.75 mm in diameter (Visicoil, IBA dosimetry, Louvain-la-neuve, Belgium) was percutaneously inserted near the tumor under the guidance of ultrasonography or CT as an internal surrogate for tumor position. We avoided implanting the marker inside the tumor to reduce image artifacts over the tumor and to prevent marker displacement. In a patient with two lesions, two markers were implanted with one marker for each of the lesions. Planning CTs were acquired one week after insertion of the marker.

The patient was placed in supine position, with both arms raised, using an individualized vacuum pillow (bodyFIX; Elekta, Stockholm, Sweden, or ESFORM, Engineering System, Matsumoto, Japan). Two sets of 4DCT and two or three sets of breath-hold CT at exhale were acquired for treatment planning using a 16-slice CT scanner (LightSpeed RT16 or BrightSpeed Elite; GE Healthcare, Little Chalfont, UK). In IBRI, a non-contrast breath-hold CT was acquired ahead of the following procedures. Then, non-contrast 4DCT image was obtained with axial cine-mode using a real-time positioning management system (Varian Medical Systems, Palo Alto, CA). The cine duration time of the scan at each table position was 6–8 s, which was longer than the maximum observed respiration period. Breath-hold CT scans were acquired using helical scanning 30 and 90 s after the start of the injection of 100 ml of iohexol

(Omnipaque 300, Daiichi Sankyo, Tokyo, Japan) at a rate of 2 ml/s. The second 4DCT scans were acquired using with the same imaging conditions as used in the first except for the contrast medium. Both 4DCT images were binned into ten respiratory phases using an Advantage Workstation (GE Healthcare) based on a phase-angle sorting method.

Planning target volume for tumor-tracking ($PTV_{tracking}$) margin definition

The $PTV_{tracking}$ was defined as the internal target volume for tumor-tracking ($ITV_{tracking}$) plus additional margins. The margins were defined individually for each patient considering the (*a*)interfractional error, which consisted of the residual set-up error, the uncertainty in fiducial marker detection, the rotational effect of the fiducial marker, and interfractional variation in the geometry of the fiducial marker and the tumor, (*b*)intrafractional baseline drift of the abdominal position detected by IR markers during irradiation, (*c*)4D modeling errors, and (*d*)mechanical errors of the gimbal system. The estimated value of the sum of *a*, and *d* was 0.5 mm. *b* was estimated 10% of the tumor motion amplitude, which was evaluated in the pre-planning 4D model. *C* was defined as the mean plus two times standard deviation from the pre-planning 4D model. The PTV margin was defined as the linear sum of these margins ($a + b + c + d$) and its minimum size was set to 5 mm in each direction. These margins were not compensated by the $ITV_{tracking}$.

Beam delivery

The patient was placed in supine position on the vacuum pillow. Set-up error was evaluated in six degrees of freedom (translations along the left-right (LR), cranio-caudal (CC), and anterior-posterior (AP) directions; and the pitch, roll, and yaw rotations) based on the bony structures by the ExacTrac X-ray system. When the rotational errors exceeded 1.5 degrees, the patient would be repositioned. The set-up correction was done in three degrees of freedom (i.e. translations only). Then, a 4D model was built for the treatment fraction. Before treatment beam irradiation was started, the kV X-ray images were used to check the position and movement of the Visicoil to ensure that they matched the predictions of the 4D model. During irradiation, the Visicoil was monitored visually using the kV X-ray imagers every second through the console display (Supplementary Fig. 2). In the case of an error > 3 mm between the predicted position of the Visicoil and the actual position monitored by the kV X-ray, the treatment beam was stopped manually. If the error > 3 mm continued in more than five successive images of kV X-ray, the 4D model was created anew to compensate for the positional error. One of radiation oncologists who were in charge of DTT-SBRT joined every treatment session to decide rebuilding a new 4D model.

Evaluation of tracking accuracy

The intrafractional prediction error was defined as the absolute difference between the detected target position (Pd) and the predicted target position (Pp). The Pd was

determined on the basis of the internal fiducial marker position, which was detected using software provided by BrainLab in the kV X-ray images. The Pp was calculated from log files acquired synchronously during treatment.

The average 95th percentiles of the absolute value of the intrafractional prediction errors were 1.1 mm (range, 0.8–1.8 mm), 2.3 mm (1.3–4.4 mm), and 1.7 mm (0.7–4.3 mm) in the LR, CC, and AP directions, respectively (Supplementary Table 2).

Evaluation of intrafractional variation

The variation of the relative position of the tumor with respect to the fiducial marker was evaluated using the contrast-enhanced four-dimensional computed tomography (4DCT) scans. For each tumor *m*, its position relative to the center of the Visicoil was measured on each respiratory phase *n*% (*n* = 0, 10, … or 90). The relative position was represented as a vector, $V_{n,m}$. Using the 50% phase images (V_{50}) as a reference, the error was defined as $E_{n,m} = V_{n,m} - V_{50,m}$. To evaluate systematic displacement during the respiratory phases, the average error of all tumors (M_n) and the standard deviations (SD_n) of $E_{n,m}$ in each phase were calculated.

$$M_n = \frac{E_{n,1} + E_{n,2} \ldots + E_{n,m}}{m}$$

$$SD_n = \sqrt{\frac{(E_{n,1} - M_1)^2 + (E_{n,2} - M_2)^2 + \ldots + (E_{n,m} - M_m)^2}{m}}$$

The root mean square (RMS) of the SD_n was also calculated to evaluate inter-patient variations.

$$\text{RMS} = \sqrt{\frac{SD_0{}^2 + SD_{10}{}^2 + \cdots + SD_{90}{}^2}{10}}$$

The means ± SDs of the intrafractional variations in the relative positions of the tumor to the fiducial marker (M_n) were 0.1 ± 0.1 mm, −0.1 ± 0.2 mm, and −0.2 ± 0.5 mm; the RMS values were 0.9, 1.2, and 1.5 mm in the LR, CC, and AP directions, respectively (Supplementary Fig. 4).

Supplementary figures

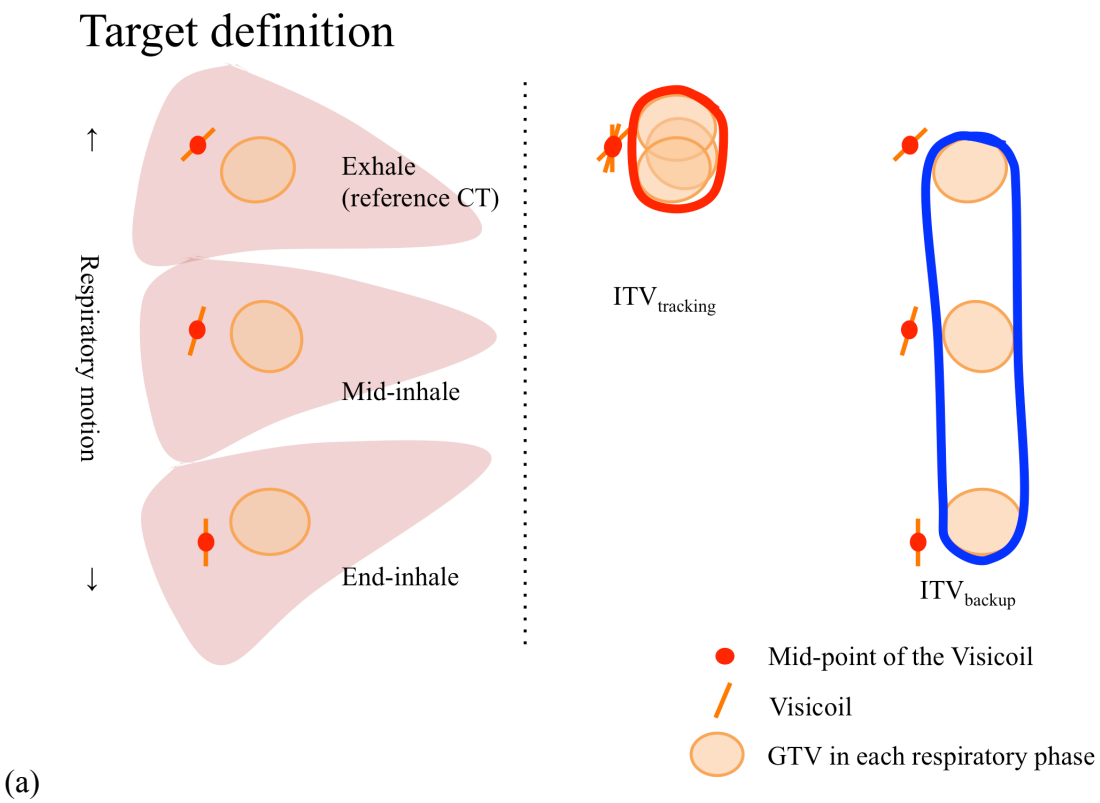

(a)

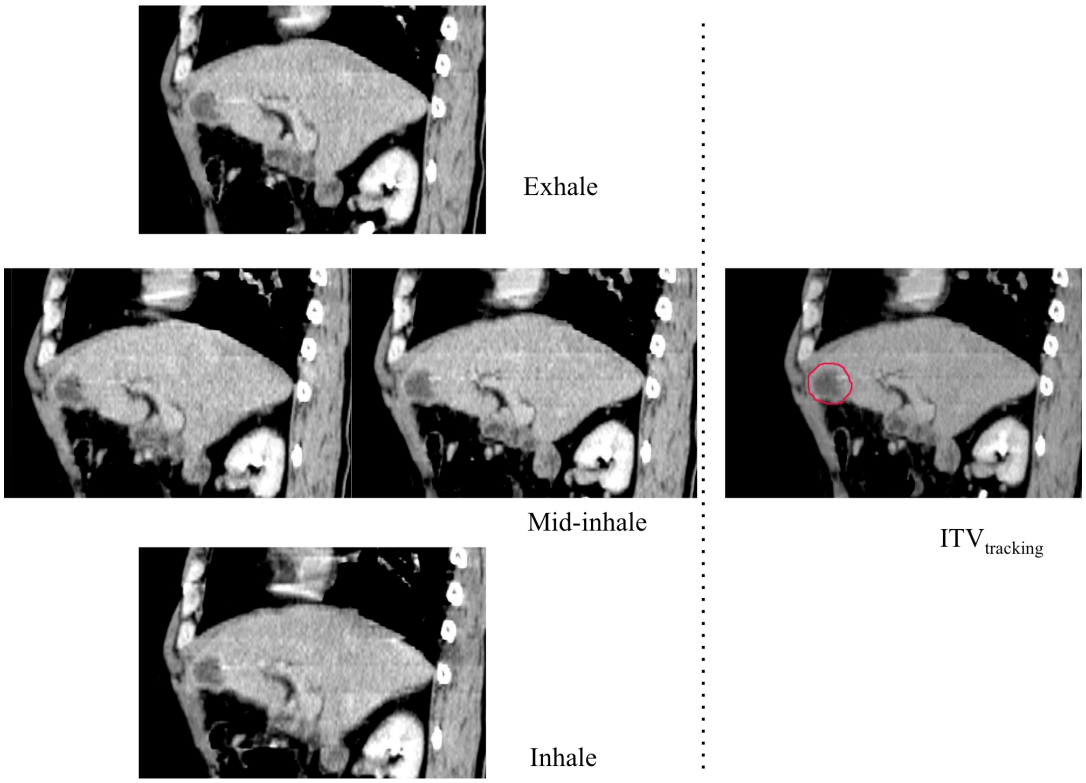

(b)

Supplementary Fig. 1 Illustration of definition of targets for dynamic tumor tracking and static plan. The liver motion and deformation, and tumor motion, deformation, and positional variation between the mid-point of the fiducial marker and the tumor during respiratory cycle were shown in the left column. The reference computed tomography (CT) was used to superimpose other phases of four-dimensional (4D) CT to delineate internal target volume for tracking ($ITV_{tracking}$). In the right column, red circles indicate the $ITV_{tracking}$ which includes gross tumor volumes (GTVs) in each respiratory phase and influence of tumor deformation, positional error due to the fiducial marker rotation, and uncertainty in the positional relationship between the tumor and fiducial marker during respiration. Blue circle indicates the ITV for static plan (ITV_{backup}) based on the motion-encompassing method (a). Actual images of contrast enhanced 4DCT. Representative phases of 4DCT are in the left column and $ITV_{tracking}$ is in the right column (b).

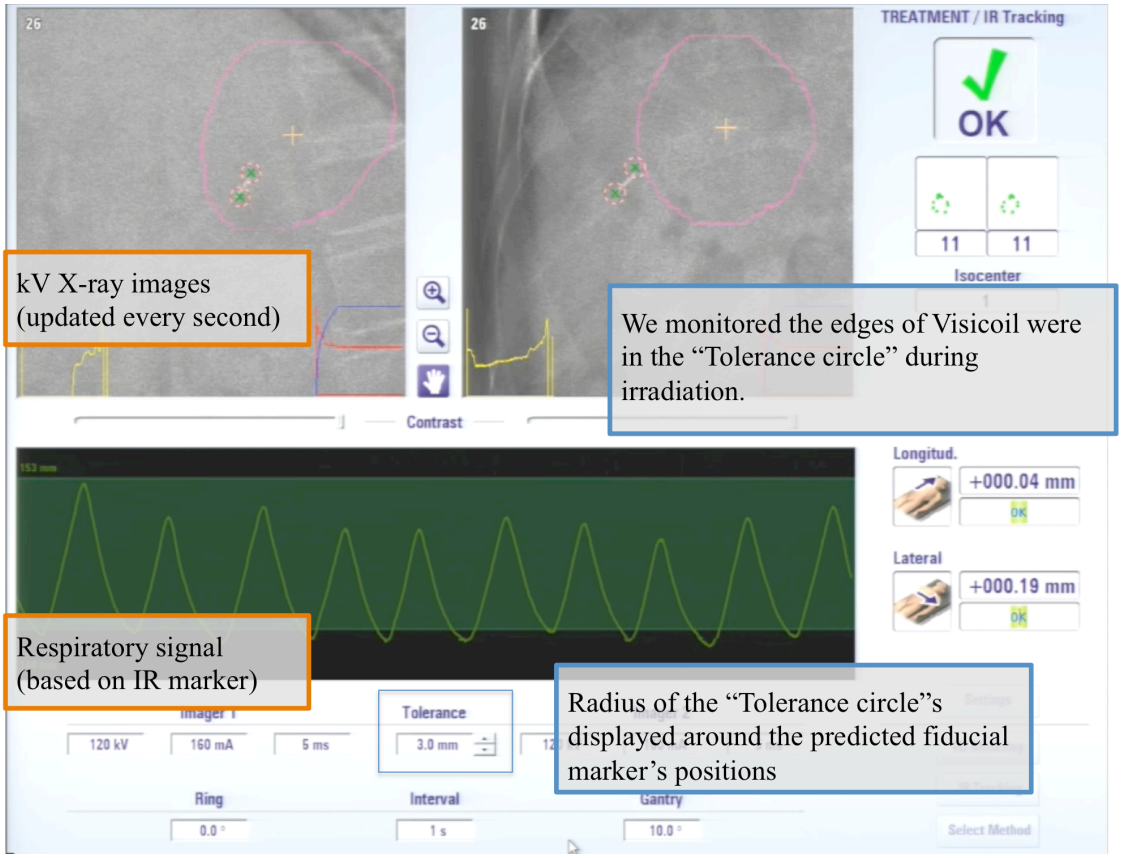

Supplementary Fig. 2 Screen shot of the Vero4DRT console during infra-red (IR) marker-based dynamic tumor-tracking irradiation. The pair of kV X-ray images were in the upper windows. Pink circles indicate the predicted positions of planning target volume, green crosses indicate the predicted position of edges of the Visicoil, and circles in dot line around the green crosses indicate "Tolerance circle"s. The respiratory signal acquired with IR markers on abdominal wall was shown in the lower window. We checked the kV X-ray images and stopped the treatment beam when the Visicoil edges deviated from the "tolerance circle".

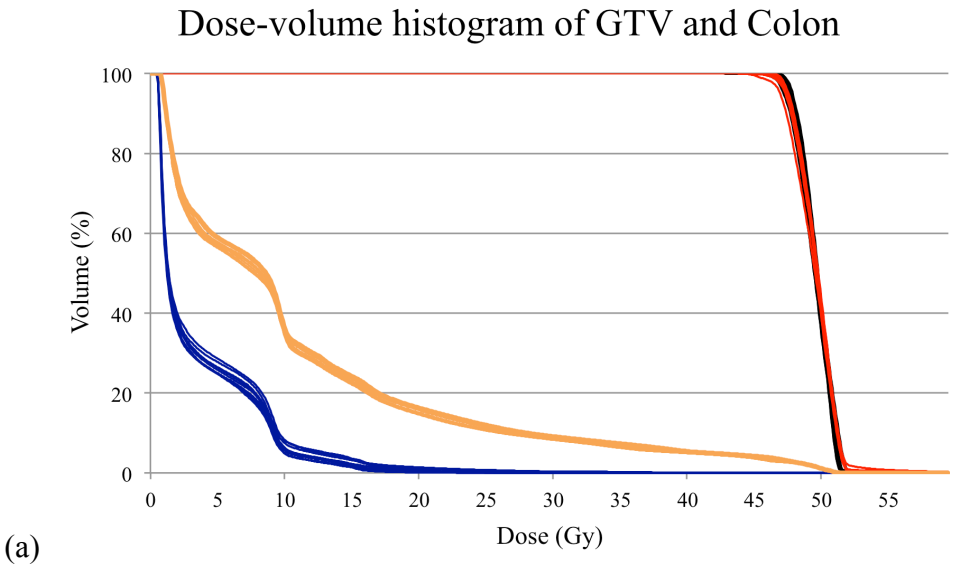

(a)

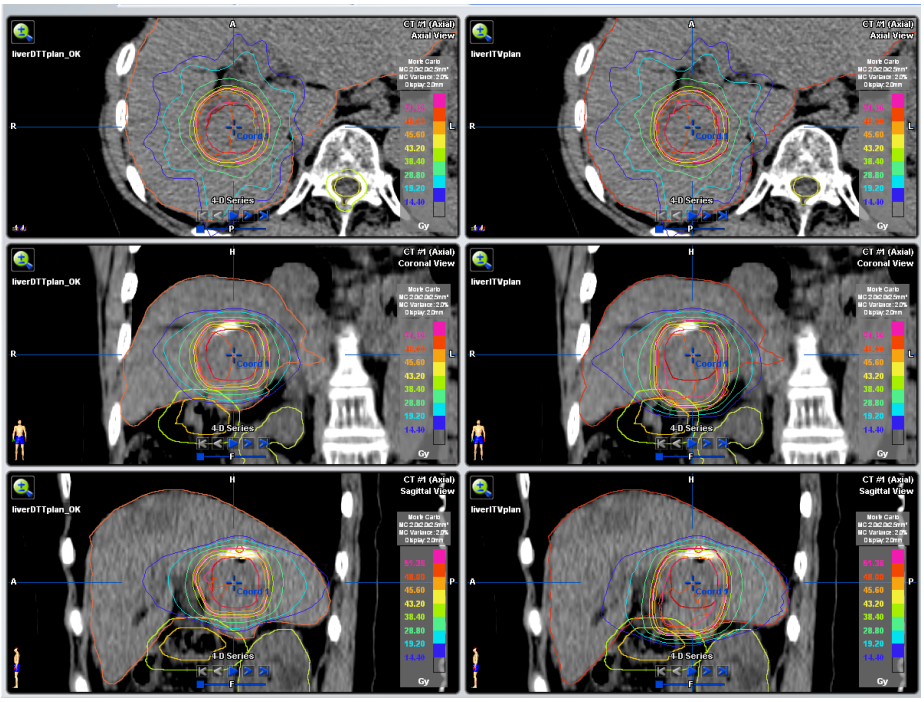

(b)

Supplementary Fig. 3 Dose-volume histogram and dose distribution of patient 4.The prescribed dose was 56 Gy. Red lines indicate the dose of gross tumor volume (GTV) in the static plan, black lines the dose of GTV in the dynamic tumor-tracking (DTT) plan, amber lines the dose of the colon in the static plan, and the blue lines the dose of colon in the DTT plan. The plural lines correspond to each respiratory phase. The maximum

dose of colon reduced from 51.7Gy in the static plan to 33.6Gy in the DTT plan (a). The dose distribution is shown in (b). Red circle indicates the GTV and yellow circle under the liver indicates the colon. Left: DTT plan. Right: static plan.

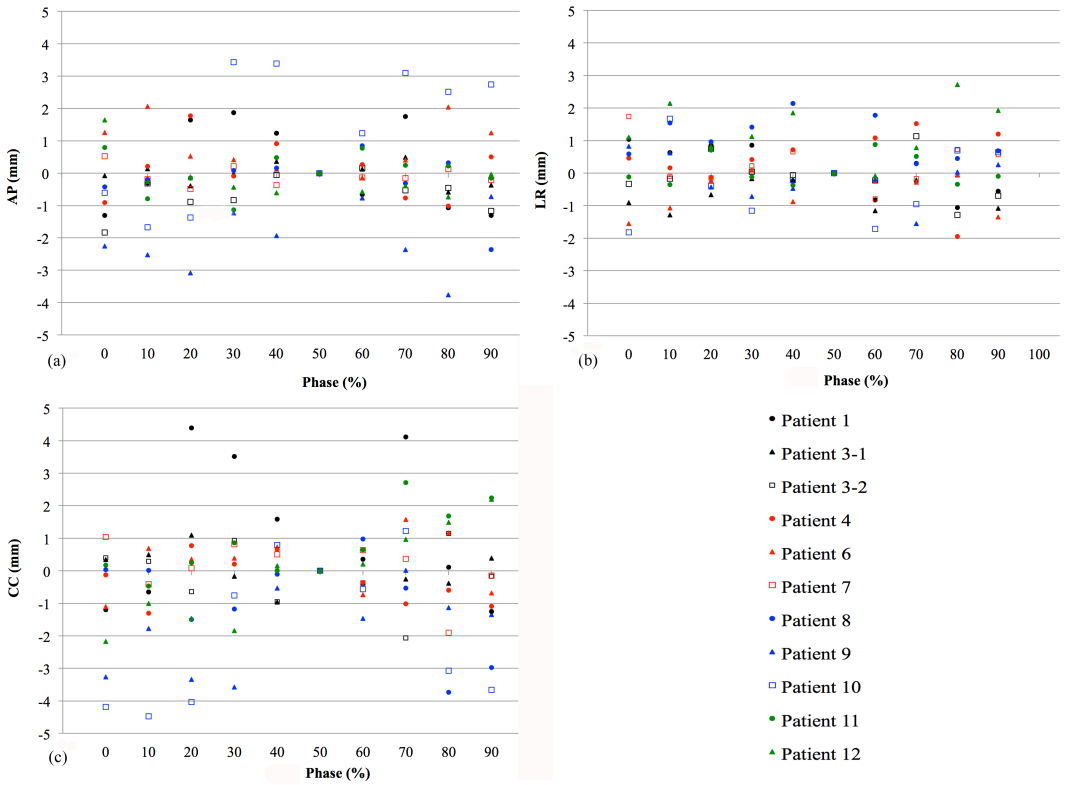

Supplementary Fig. 4 The position of the tumor center relative to the center of the Visicoil on *n*% of the phase images (*n* = 0, 10, … or 90) of each tumor in the anterior-posterior (AP) (a), left-right (LR) (b), and cranio-caudal (CC) (c) directions. These different markers correspond to the each of tumors.

Supplementary tables

Supplementary Table 1 Treatment time per fraction, the number of times a 4D model was created.

Patient	Treatment time (min)	Number of 4D models
1	36, 42, 41, 35	2, 3, 2, 2
3	34, 35, 18, 20, 34, 18, 45, 25	2, 2, 1, 1, 2, 1, 3, 1
	48, 48, 24, 21,	1, 3, 1, 1
4	29, 25, 24, 25	2, 1, 1, 1
6	32, 30, 19, 23, 25, 20, 23, 17	2, 1, 1, 1, 1, 1, 1, 1
7	32, 33, 31, 30	2, 2, 2, 2
8	25, 25, 23, 22, 24, 25, 22, 27	1, 1, 1, 1, 1, 1, 1, 1
9	33, 41, 25, 34, 24, 43, 44, 26	2, 3, 1, 3, 2, 3, 3, 1
10	26, 33, 24, 20, 24, 26, 33, 21	1, 2, 1, 1, 1, 1, 2, 1
11	23, 29, 20, 21, 22, 29, 21, 21,	1, 2, 1, 1, 1, 2, 1, 1
12	25, 22, 32, 23	1, 1, 2, 1

The treatment time included patient set-up, building the 4D model, and beam delivery. The number of 4D models built per treatment fraction was one in 42 fractions, two in 19 fractions, and three in 7 fractions.

Supplementary Table 2 Summary of the absolute values of the tumor prediction errors.

	Mean error (mm)			95th percentile error (mm)		
Patient	LR	CC	AP	LR	CC	AP
1	0.3	1.9	1.7	0.8	4.4	4.3
3	0.7	1.1	0.6	1.8	2.8	2.1
	0.4	1.1	0.5	1.0	2.6	1.5
4	0.3	0.6	0.6	0.8	1.8	1.2
6	0.4	1.0	0.7	1.1	2.2	2.0
7	0.5	0.9	0.9	1.4	2.2	2.1
8	0.8	1.0	0.5	1.8	2.3	1.2
9	0.2	0.0	0.3	0.9	2.1	1.7
10	0.5	0.9	0.2	0.9	1.8	0.9
11	0.5	0.7	0.4	0.8	1.3	0.7
12	0.5	1.2	0.4	0.8	2.1	0.8

Abbreviations; LR: left-right, CC: cranio-caudal, AP: anterior-posterior.